Event Horizon Telescope
Memo Series

EHT Memo 2018-CE-01

Calibration & Error Analysis WG

James Clerk Maxwell Telescope Calibration Memo Time dependence of the aperture efficiency and DPFU

S. Issaoun[1], H. Falcke[1], P. Friberg[2], M. Janssen[1], R. Tilanus[1] and J. Wouterloot[2]

Jan 2, 2018 – Version 1.0

[1]*Department of Astrophysics/IMAPP, Radboud University Nijmegen, 6500 GL Nijmegen, the Netherlands*
[2]*East Asian Observatory, 660 N. A'ohōkū Place, University Park, Hilo, HI 96720, USA*

Abstract

We investigate a time dependence in the aperture efficiency of the James Clerk Maxwell Telescope (JCMT). This time dependence indicates a loss of efficiency for the telescope during the daytime hours on Hawaii most likely due to the dish surface heating from the Sun. We fit the nighttime dependence as a constant aperture efficiency and the daytime dependence as a negative Gaussian (absorption curve) aperture efficiency as a function of local time on Hawaii (HST). This dependence propagates to the Degree Per Flux Unit (DPFU) scaling factor needed for the station-based amplitude calibration as part of the Event Horizon Telescope. The JCMT observed a number of hours in the daytime during the 2017 campaign, therefore the daytime contribution is a necessary factor to be included in the ANTAB tables for a priori amplitude calibration.

1 Method

The JCMT staff provided aperture efficiency measurements for the telescope at 230 GHz using planet calibrators. Over a hundred different measurements[3] were performed from 2006 to 2017 with Mars, Jupiter and Uranus, presented in Fig. 1. Clear outliers from the general trend were flagged - efficiencies below 0.3 and above 0.7 - before any fit was attempted on the data. We separated the nighttime and daytime data points based on average sunrise and sunset times on Hawaii: the daytime measurements were chosen to be all points measured between 6 HST (sunrise) and 19 HST (sunset), all other points were interpreted as part of the nighttime trend. The conversion from local Hawaii time to UT is UT = HST + 10.

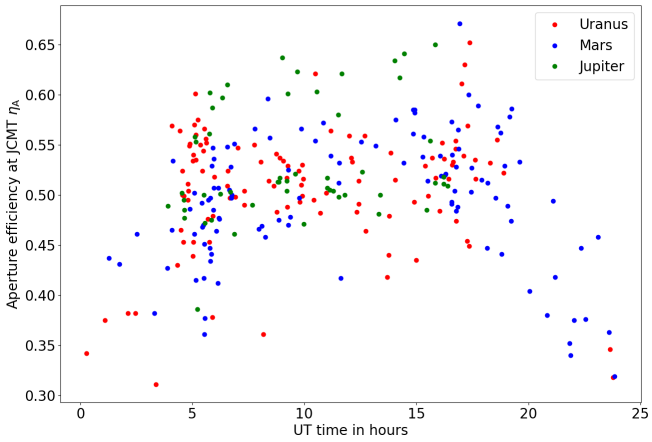

Figure 1: Aperture efficiency measurements from 2006 to 2017 at the JCMT.

2 Results

2.1 Nighttime fit

The nighttime aperture efficiency is expected to be very stable due to the dish having cooled down. We thus fitted the nighttime data points with a constant aperture efficiency value. The nighttime efficiency obtained is:

$$\eta_{\mathrm{A,night}} = 0.516 \pm 0.054 \quad (1)$$

The uncertainty on the nighttime value is determined by taking the standard deviation on the mean of the measurements approximated as a Gaussian distribution, as in Fig. 2. The median of the measurements is 0.514, which only differs from the mean by 0.04σ.

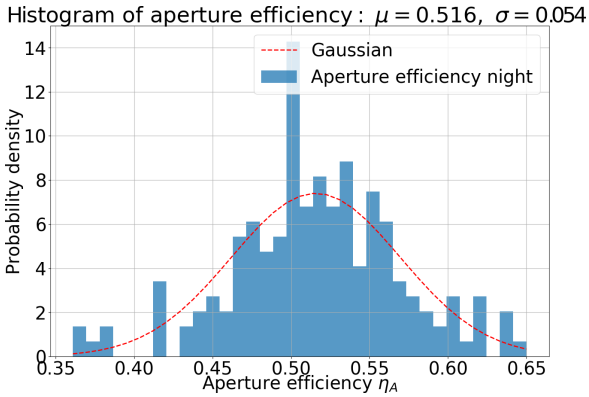

Figure 2: Histogram of the nighttime measurements approximated as a Gaussian distribution.

The measurements of aperture efficiency before 6 HST and after 19 HST correspond to the UT range of 5-16 UT, where most of the observations with the JCMT are performed in the EHT schedules.

2.2 Daytime fit

The daytime aperture efficiency trend showed a dip in efficiency during the day, due to the dish surface being affected by heating from the Sun and e.g. an expansion of the main support pillars of the backing structure. This trend is approximated as a negative Gaussian, and fitted to the daytime measurements. The daytime efficiency function is written as follows, where x_{HST} is the local time in the daytime range and the fit parameters are presented in Table 1:

$$\eta_{\mathrm{A,day}} = 1 - Ae^{-\frac{(x_{\mathrm{HST}}-x_0)^2}{2\sigma^2}} \quad (2)$$

Table 1: Daytime aperture efficiency fit parameters.

parameter	value
A	0.599 ± 0.014
x_0	13.55 ± 0.21
σ	9.16 ± 0.45

[3]The method used to derive the measurements is outlined in the *A priori Calibration Memo by Issaoun et al. (2017)* and will not be explained here. See appendix for details on planet parameters.

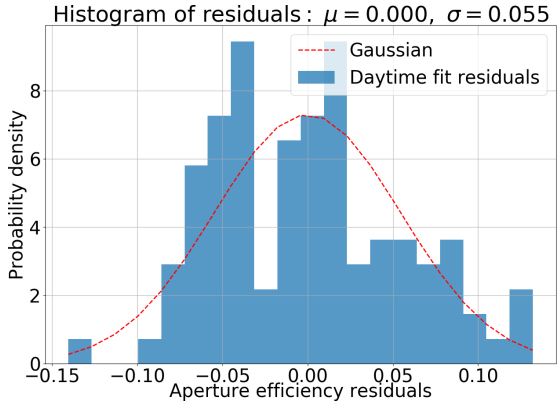

Figure 3: Histogram of the daytime measurements approximated as a Gaussian distribution.

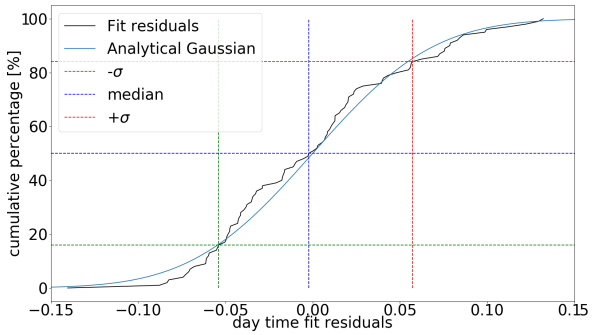

Figure 4: Cumulative sum plot of the fit residuals compared to the cumulation of an analytical Gaussian distribution.

To determine the uncertainty on the fit as a whole, we subtracted the fitted aperture efficiencies from the measured values at every daytime HST and the residuals were used for error estimation. Approximating the residual distribution as a Gaussian, a standard deviation of $\sigma = 0.0547$ was found, as shown in Fig. 3. However, the distribution seems to have two peaks and does not look entirely Gaussian. We thus performed an additional analysis using cumulative statistics.

The standard deviation from the median of the residuals was determined from the cumulative sum of the residuals, shown in Fig. 4. Here the median also lies very close to the mean of zero, and we see a broad agreement between the cumulative trend of the fit residuals and the analytical Gaussian. Therefore it seems reasonable to use the Gaussian standard deviation as the uncertainty on the fit. The average uncertainty from the positive and negative standard deviation from the median in the cumulative plot is $\sigma_{\text{avg}} = 0.0554$. This value is taken as the overall uncertainty on the time-dependent negative Gaussian fit for the daytime aperture efficiency. Fig. 5 shows the two final fits as a function of local time on Hawaii (HST).

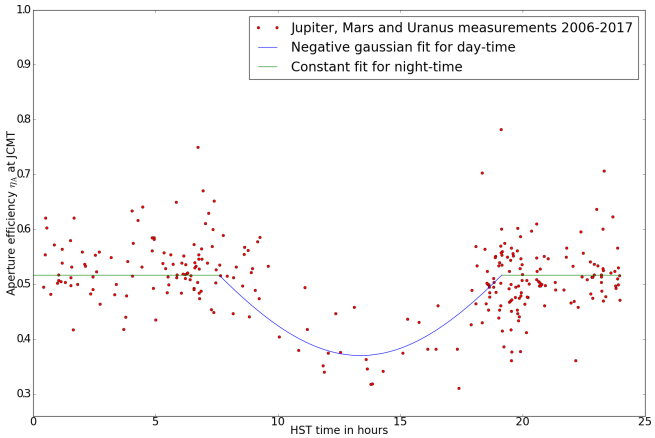

Figure 5: Daytime and nighttime fits to the aperture efficiency measurements.

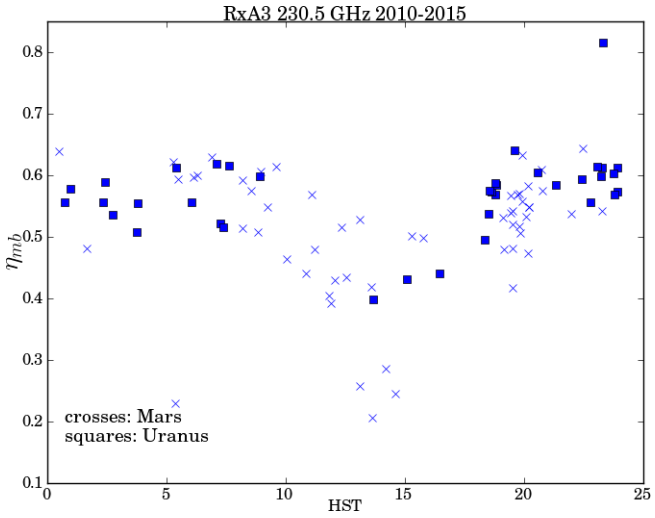

Figure 6: Main beam efficiency measurements at the JCMT (with the RxA3 receiver) versus Hawaii Standard Time for all observations between 2010 and 2015.

A similar behavior of the main beam efficiency for the telescope, shown in Fig. 6, has been observed by JCMT staff using measurements between 2010 and 2015. They have found that there is a significant decrease in the main beam efficiency during the day, and that this decrease is less on a cloudy day when the Sun has less effect on the surface of the dish.

Comparing our fits to the main beam efficiency findings, the points on the lower envelope of the daytime dip are likely due to clear-sky days (with the Sun lowering the efficiency) and the points on the upper envelope are due to cloudy days. In April 2017, daytime weather on Hawaii varied from mildly cloudy to clear in the afternoons, thus the error bud-

get is expected to be representative of varying observing conditions at the telescope during EHT observations.

2.3 The time-dependent DPFU

The DPFU for the JCMT carries forward the time dependence of the aperture efficiency. We have a constant nighttime DPFU and a daytime negative Gaussian fit DPFU[4], where k is the Bolzmann constant and $A_{\rm geom}$ is the geometric area of the JCMT assuming a diameter of 15 meters:

$$\mathrm{DPFU_{night}} = \frac{A_{\rm geom}}{2k} \times \eta_{\rm A,night} = 0.03304 \pm 11\% \quad (3)$$

$$\mathrm{DPFU_{day}} = \frac{A_{\rm geom}}{2k} \times \eta_{\rm A,day} = 0.0640 \times \eta_{\rm A,day} \pm 14\% \quad (4)$$

3 Conclusion

The time-dependent trend for the aperture efficiency of the JCMT seems very stable through the years and well-constrained by the two different fits. The scatter in the measurements, used here to derive an error budget for the JCMT, are likely due to variations in the quality of the observing conditions and telescope performance and likely not due to a changing dish surface. The error budget however is expected to be representative of varying observing conditions at the telescope during EHT observations. Provided that no changes are made to the JCMT dish surface, these two relations should be suitable for practical use in future observing runs.

The cause of this dip in efficiency, however, remains to be explained. At the JCMT, thermal models of the antenna (during the design and later by Fred Baas) predict surface distortion caused by thermal gradients in the dish backup structure originating from changes in temperature in the building. The heavier elements in the backup structure heat up (or cool down) much slower than lighter pieces, generating these temperature gradients. The theoretical implications of the dish distortion have been studied but never measured experimentally and were not pursued after the telescope stopped daytime observing, although the JCMT still keeps a temperature monitoring system.

Another effect on the efficiency is an absolute temperature change in the panels of the dish: the panels are made of thin aluminium layers on a stiff foam substrate, with different expansion coefficients, so the panel shapes are expected to change with temperature. This effect is aggravated if the surface is under direct sunlight, such that the panels heat up more than the building itself. Direct sunlight on at least part of the dish is also known to cause rapid focus changes.

The telscope building heats up during the day and telescope staff generally aim to open the dome in the afternoon to speed up the cooldown and limit the effect of dish distortion in the early evening. Therefore the time gap between the opening of the dome for cooldown and the first observations also matters in the estimation of the aperture efficiency. The seeing is also generally worse in the afternoon, worsening telescope performance.

While the fits presented here are of good practical use, it is generally preferable to complement them with direct efficiency observations of planet calibrators and a monitoring of observing conditions such as: when the dome was opened, how much cooldown time before the first observations, possible effects of direct sunlight on the dish, clear versus cloudy afternoons etc.

[4]The relative error on the DPFU includes a 5% uncertainty on the planet brightness temperatures used for the planet calibration measurements added in quadrature to the aperture efficiency error estimates.

Appendix: JCMT planet calibration

Overview of planet brightness temperatures used at the JCMT by M. Currie.
Filename: `scuba2.txt`

scuba2.txt

```
 Number of filters defined =  5
 Number beams defined per filter =  2

 NF  Wavelength    Freq.  Width  HPBW  HPBW2    A1    A2
  1  850           350.0   30.0  13.0   48.0  0.98  0.02
  2  450           677.0   30.0   7.9   25.0  0.94  0.06
  3  1300          234.5    1.0  20.0    0.0  1.00  0.00
  4  868           345.8    1.0  14.0    0.0  1.00  0.00
  5  434           691.5    1.0   8.0    0.0  1.00  0.00
  6                  0.0    0.0   0.0    0.0  0.00  0.00
  7                  0.0    0.0   0.0    0.0  0.00  0.00

 Planetary temperatures and errors:

              Mars         Jupiter      Saturn       Uranus       Neptune
 850          0.0   0.0  163.8   4.0  124.3   5.0   82.7   1.0   78.1   5.0
 450          0.0   0.0  148.5   5.0  111.0   5.0   68.4   0.5   65.6   3.0
1300          0.0   0.0  170.0   5.0  133.0   5.0   96.9   0.5   95.2   0.5
 868          0.0   0.0  163.8   4.0  124.3   5.0   86.6   0.0   71.8   0.0
 434          0.0   0.0  148.5   5.0  111.0   5.0   70.2   0.0   64.2   0.0
              0.0   0.0    0.0   0.0    0.0   0.0    0.0   0.0    0.0   0.0
              0.0   0.0    0.0   0.0    0.0   0.0    0.0   0.0    0.0   0.0

Notes these are revised numbers as of 20 Apr 2012:

The Uranus and Neptune brightness temperatures are from Moreno, R. 2010, "Neptune and Uranus planetary brightness
temperature tabulation, available from ESA Herschel Science Centre." The errors in brightness temperature are simply
an estimate from the variation over the filters and are not used by FLUXES. The Herschel calibration data indicate
that the SCUBA-2 filters are coincident with strong absorption lines. A more detailed analysis of the SCUBA-2 filters
in combination with the Neptune brightness temperatures is required before Neptune should be used for calibration.

The Jupiter brightness temperatures are obtained from the measurements of Griffin et al. 1986, Icarus 65, 244.
The errors in brightness temperatures are the rms internal errors of the observations. For MJD's between 46040
through 50000 the Martian temperatures are derived from the model developed by  Wright 1976, Ap.J., 210, 250.
Outside these MJD's i.e., in particular after 10 October 1995 a simplified model of a rotating cratered asteroid is
used Wright, E. L, 2007, astro-ph/0703640v1. Since the results for Mars are derived from models no errors are quoted;
however the Martian brightness temperatures are probably uncertain at the 5% level and this uncertainty must be added
to obtain the absolute errors. Over the interval for which both the original Wright model and the simplified model are
valid, the differences in brightness temperatures have an rms error of 0.13 K i.e. negligible. The flux densities for
Saturn are for the planetary disk only; an additional flux is expected when the rings present an open aspect, and at
such times Saturn should not be used as a calibration object. Individuals using these data in published works should
reference the appropriate papers as noted above. The filter frequencies are the effective frequencies for 1mm of water
vapour. These are the SCUBA-2 filters.

1300, 868, and 434 micron 234.5, 345.8, 691.5 GHz are for heterodyne receivers. Saturn, Mars copied from scuba.dat;
Uranus and Neptune from ESA4 values for 234.5 GHz are CO in LSB as normally observed with RxA3.
```